Pion double charge exchange on ^{56}Fe at $T_\pi = 400$ MeV

D. A. Smith, H. T. Fortune, J. M. O'Donnell,* J. D. Silk,† B. Gluckman, R. Crittenden, and N. Claytor‡
University of Pennsylvania, Philadelphia, Pennsylvania 19104

C. L. Morris and J. A. McGill§
Los Alamos National Laboratory, Los Alamos, New Mexico 87545
(Received 11 November 1992)

Data were measured for pion double charge exchange on ^{56}Fe at T_π =400 MeV and three laboratory angles: 0°, 10°, 20°. Angular distributions were measured for the double isobaric analog state, the analog of the giant dipole resonance, and the giant dipole built upon itself. The excitation function of each of these resonances is discussed. Evidence is found for separate J^π components of the double dipole resonance, and cross sections of these components are extracted.

PACS number(s): 25.70.Gn, 24.30.Cz

INTRODUCTION

The isovector giant dipole resonance (GDR) is a well known structure and has been studied on many nuclei using photonuclear reactions [1]. In recent years it has been recognized that the pion can be a useful probe to populate this resonance [2,3]. The pion is spinless, with low mass, favoring low angular momentum transitions in inelastic scattering. Also, use of charge-exchange reactions selects out isovector transitions. In pion double charge exchange (DCX) the GDR built on special excited states has been measured in nuclei across the mass table [4–7]. The resonances that have been studied using DCX are the analog of the GDR, i.e., the dipole analog (DA) and the GDR built upon itself, the double dipole resonance (which we abbreviate as DD).

All published DCX results up to now have been at only one beam energy, 292 MeV. In this work we have made observations of these states at T_π = 400 MeV, in order to obtain information on their excitation functions. We were also able to observe the double isobaric analog state (DIAS), providing further information on the excitation function of this state. To identify these resonances a three-point angular distribution was measured, and the measured cross sections are compared to theoretical calculations.

The GDR is excited by a pure 1^- transition, which produces a characteristic angular distribution. The isobaric analog state is by its nature reached by a 0^+ transition. This combination will give the DA [4] the same type of angular distribution as the GDR [2]. The DD is reached by two 1^- transitions, giving this resonance an angular distribution that is a superposition of 0^+ and 2^+ shapes [5]. Evidence of this resonance in the data on iron would be a peak at forward angles and peaking again at 20°. In most nuclei these 0^+ and 2^+ components of the DD will be separated somewhat in excitation energy [8]. As we shall see, the data measured in this work show evidence of such a separation.

EXPERIMENT AND DATA ANALYSIS

This experiment was performed at the High-Energy Pion Channel (P^3) of the Clinton P. Anderson meson physics facility (LAMPF). The experiment used the large acceptance spectrometer (LAS) with what is now the standard DCX small-angle setup [9], a 400-MeV π^+ beam with a dispersed tune, and a natural iron target, 7.5 by 7.5 cm and 2.50 g/cm^2 in areal density. Electrons were rejected using an isobutane-gas velocity-threshold Cherenkov detector in the focal plane. Accidental and muon events from π decay were rejected in software by ray tracing of the particle path. The experiment was designed to observe the DA at high incoming beam energy, and pions of this Q value were placed in the center of the spectrometer acceptance. The momentum acceptance of the spectrometer was such that the DIAS and the DD could both be observed in each measurement. The acceptance of the device at different momenta was measured by inelastic scattering on carbon and sweeping an excited peak across the focal plane. For absolute normalization, elastic scattering was measured on hydrogen and compared to known cross sections. Three angles were measured: 0°, 10°, and 20°, the 0° measurement corresponding to a mean scattering angle of 2°. The data are

*Present Address: Los Alamos National Laboratory, MS H841, Los Alamos, NM 87545.
†Present Address: Institute for Defense Analysis, 1801 N. Beauregard, Alexandria, VA 22311.
‡Present Address: Physics Department, Notre Dame University, South Bend, IN 46556.
§Present Address: SSC Laboratory, 255 Beckleymeade Ave., Dallas, TX 75237.

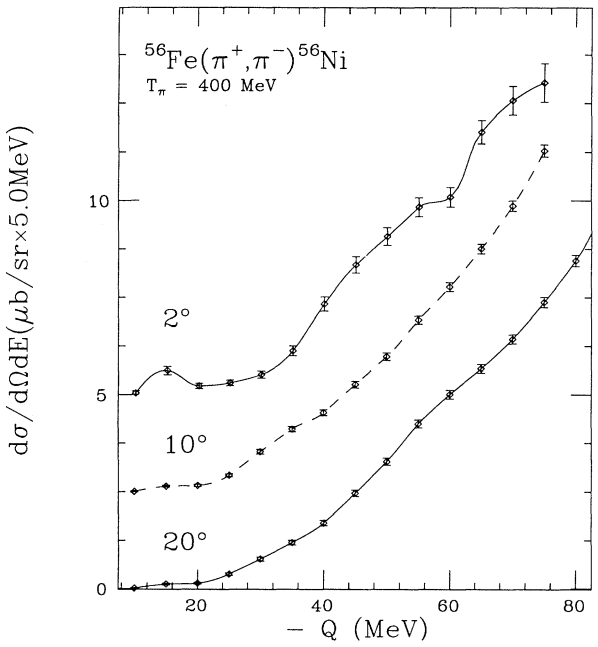

FIG. 1. Spectra of outgoing pions from $^{56}Fe(\pi^+,\pi^-)^{56}Ni$ at T_π = 400 MeV, plotted in 5-MeV bins. The lines shown are to guide the eye and are not theoretical fits. The 10° data have been offset by 2.5 μb/sr and the 2° data by 5 μb/sr.

displayed in Fig. 1, with a coarse (5 MeV) binning. The lines connecting the data points are to guide the eye and are not the results of a theoretical fit.

The main feature of these data is an increase in cross section with increasing negative Q value, arising from the pion DCX background. This background has a slowly varying angular dependence, and any structures above this background will show up in an angular distribution. A way to observe these structures is to examine the angular dependence at each Q value for a very rough binning. This binning was done for the current data and the results are plotted in Fig. 2. At low Q value the data exhibit an angular distribution shape that is characteristic of a 0^+ transition, as expected for the DIAS. It lies at −15 MeV in the Q value, which is consistent with other observations [10]. At a more negative Q value the structure of the data changes to a 1^- shape, in the region of the DA. It is at 35 MeV and has a width of about 5 MeV, consistent with other observations of the DA in DCX [6]. This diagram gives an idea of the locations of the DIAS and the DA resonances. The structure of the DD above the background is not so easy to observe, and more sophisticated peak shape fitting is needed. The DD has been observed in many nuclei around 50 MeV [7], and so a peak was fitted in this region.

The data with these best fits are given in Fig. 3. The background was fitted with a third-order polynomial in Q. The DIAS was fitted with a peak shape that was determined from elastic scattering. The resonances involving the GDR were fitted with Lorentzian peak shapes folded with the reference peak shape found from elastic scattering. The peak shapes and Q values for each resonance have been constrained to be the same at all angles. The cross sections found from these fits are listed in Table I.

DISCUSSION OF THE DATA

The angular distributions of the DIAS and the DA are plotted in Fig. 4. The data presented here are compared to calculations with a distorted-wave, coupled-channels code NEWCHOP [11]. For the nuclear radius and diffusivity parameters we used results of measurements of the nuclear charge density on ^{56}Fe found from electron scat-

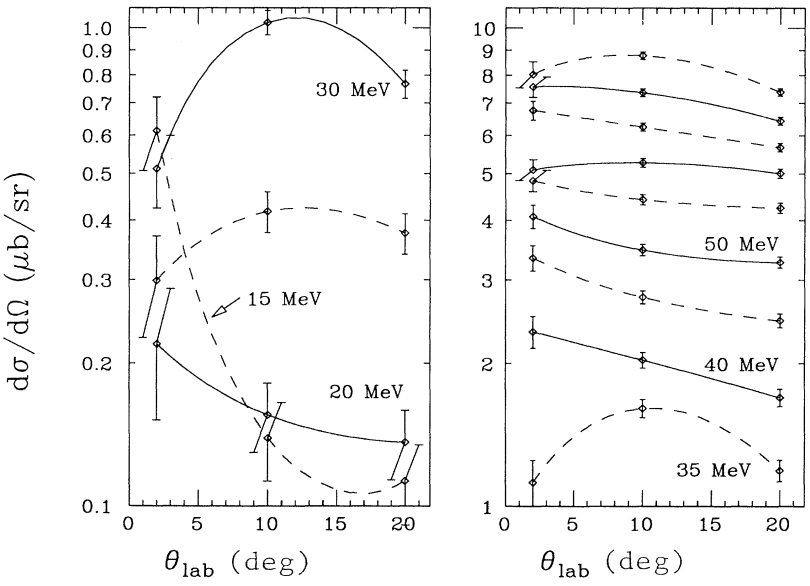

FIG. 2. Angular distributions of each 5-MeV bin shown in Fig. 1. The $-Q$ values of a few bins are marked on the plot. The lines joining the points are to guide the eye and are not theoretical fits. At −15 MeV the distribution has a 0^+ shape, because of the DIAS. The angular distributions show a clear 1^- shape between 30 and 35 MeV, where the DA is located.

TABLE I. Cross sections, energies, and widths measured in ^{56}Fe(π^+,π^-). The DIAS was fitted with a reference peak shape found for elastic scattering, and no additional width was needed. The dipole resonances were fitted with Lorentzian peak shapes with the listed widths folded with the reference peak shape.

State	$-Q$ (MeV)	Γ (MeV)	$d\sigma/d\Omega$ (μb/sr)		
			2°	10°	20°
DIAS	16.0 ± 0.2		0.55 ± 0.11	0.13 ± 0.02	0.11 ± 0.02
DA	33.1 ± 0.7	5.4 ± 1.8	< 0.32	1.03 ± 0.11	0.23 ± 0.11
DD	51.3 ± 0.5	13.9 ± 1.5	8.8 ± 0.6	1.9 ± 0.2	2.7 ± 0.3

tering [12] and made the assumption that the neutron density was the same as the charge density. The parameters used for the calculations on ^{56}Fe are listed in Table II. The NEWCHOP calculations for the DIAS fit the small-angle data well, but underpredict the cross section at 20°. The calculation for the DA fits the shape of the data quite well. We discuss the magnitudes of the calculations later.

The angular distribution of the DD is given in Fig. 5. Because the state is a superposition of 0^+ and 2^+ resonances, calculations were done for each J^π component. The two different calculations are shown in the figure, and the relative magnitude of each has been fitted to the data. The sum is shown as the solid line. The relative renormalizations are equal within errors, implying that the 0^+ and 2^+ components of the resonance are of equal strength. The 10° datum is below the calculation for this point, probably because of the difficulty of background subtraction at such high excitation. The pion DCX background is not well understood, and has no theoretical prediction of its shape and magnitude. The background at 10°, where the DD is at its minimum, is probably being oversubtracted. Better statistics at high excitation would be needed to help establish the background.

We have attempted to do parameter-free calculations for DCX, using strengths constrained to fit SCX cross sections. There are no SCX data on ^{56}Fe, but there exist data on ^{60}Ni, which is a comparable nucleus. The isobaric analog state (IAS) has been measured at several energies in SCX on ^{60}Ni [13–15]. Results of those measurements are displayed in Fig. 6, along with calculations done with NEWCHOP for each of these energies. The nuclear radius and diffusivity for ^{60}Ni as measured from electron scattering were used for these SCX calculations, which differ slightly from those of ^{56}Fe. These parameters are listed in Table II. The magnitudes of these calculations were fitted to the data to find the strength parameter β, assumed to be independent of energy. Calculations above 425 MeV could not be done, as this energy lies outside the limitations of the optical model used

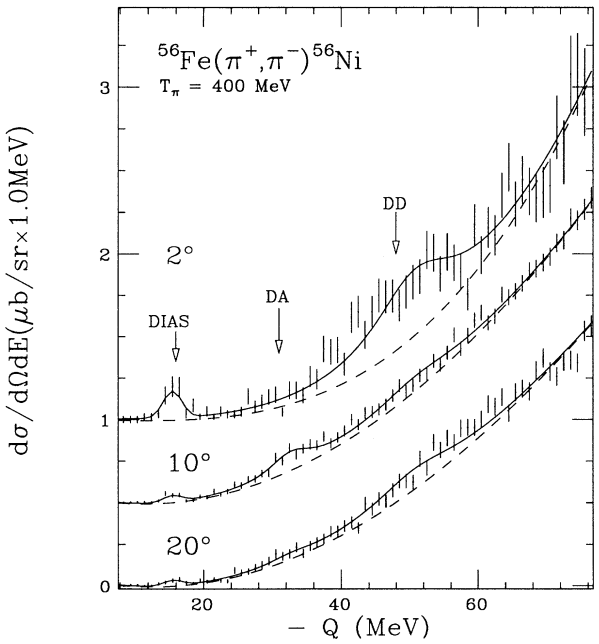

FIG. 3. DCX data in 1-MeV bins with theoretical fits. The background is shown as a dashed line and was fitted as a third-order polynomial. The DIAS at −16 MeV was fitted with a reference peak found in elastic scattering. The dipole resonances were fitted with Lorentzian peak shapes folded with the reference peak shape. The 10° data have been offset by 0.5 μb/sr and the 2° data by 1 μb/sr.

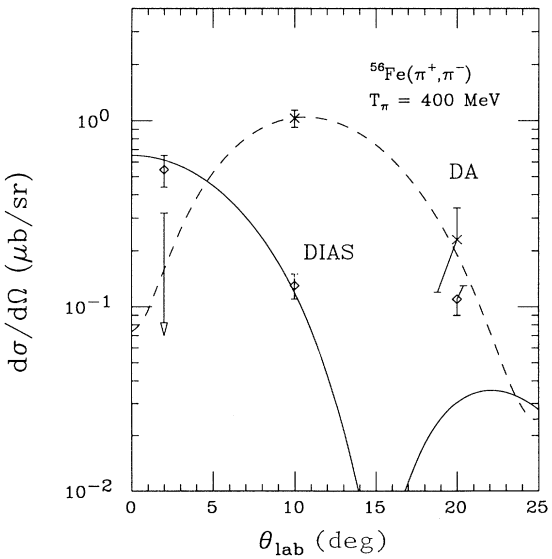

FIG. 4. Angular distributions for the DIAS and DA. The curves plotted are theoretical calculations done with NEWCHOP and fitted to the data.

TABLE II. Values of Columb radius, nuclear radius, and diffusivity of ^{56}Fe and ^{60}Ni found from electron scattering.[a]

Nucleus	$(r^2)^{1/2}$ (fm)	R (fm)	a (fm)
^{56}Fe	3.801	4.111	0.558
^{60}Ni	3.796	4.489	0.537

[a]Reference [12]. The data from electron scattering were fitted to a two-parameter Fermi form for the nuclear charge density. This information was used for the NEWCHOP calculations shown in this work.

in the code. The calculated energy dependence of the IAS using the best fit energy-independent β is shown in the figure as a solid line. The energy dependence of the data is also compared to the square of the pion momentum, shown as a dashed line in the figure. The energy dependence of the cross section for SCX to the giant dipole resonance on ^{60}Ni is exhibited in Fig. 7 [15], also with a calculation done for this resonance using NEWCHOP. This calculated cross section used a strength parameter for this state which was fitted to the data in the same method as for the IAS. The data are also compared to a k^2 dependence which is shown in the figure as a dashed line.

The β parameters for the IAS and GDR in SCX can be used to calculate the cross sections for DCX to observed states. Calculations for the DIAS in ^{56}Fe were done using NEWCHOP and the parameter β fitted to the SCX IAS data on ^{60}Ni. The results of this calculation for the DIAS are compared to DCX data [8,16–18] in Fig. 8. The limitations of the optical model restrict the calculation to below 400 MeV. The magnitude of the calculated DIAS cross sections is about right, but the predicted energy dependence is in poor agreement with the data. Such a failure to fit the energy dependence is a common feature of the DIAS studies. Both data and calculation exhibit a sharp increase in magnitude, and then a flattening of strength above 300 MeV. This is in contrast to the k^2

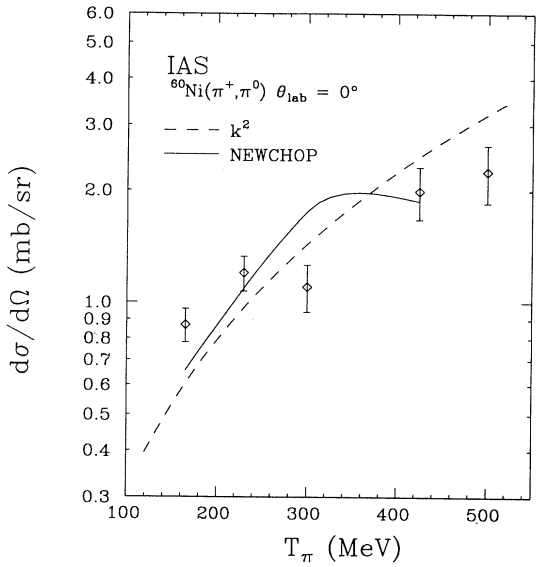

FIG. 6. Excitation functions of the isobaric analog resonance observed in single charge exchange on ^{60}Ni [13–15]. The solid curve uses NEWCHOP calculations for the energy dependence, whereas the dashed curve is k^2 fitted to the data.

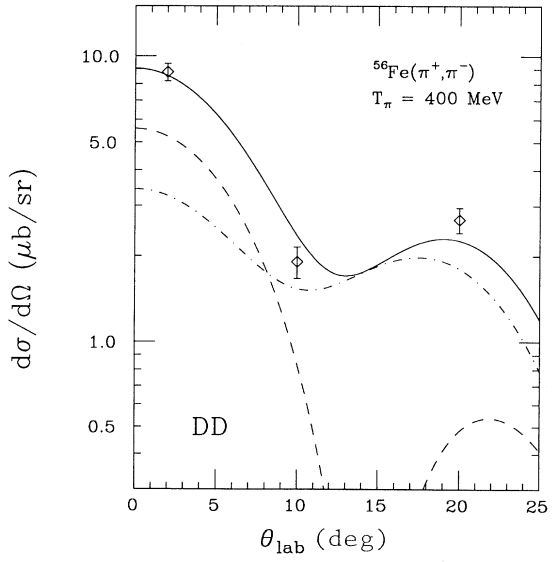

FIG. 5. Angular distribution of the DD data. The dashed curve is the NEWCHOP calculation to the 0^+ member of this state; the dot-dashed curve is the calculation for the 2^+ member. These curves have been summed and fitted to the data, and this fit is shown as the solid curve.

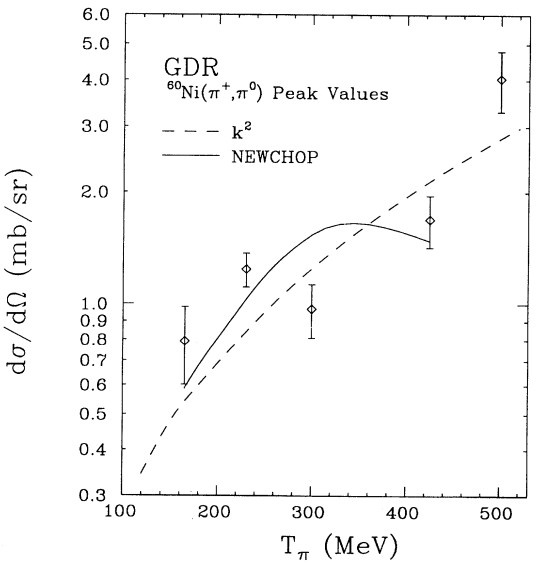

FIG. 7. Excitation functions of the giant dipole resonance observed in single charge exchange on ^{60}Ni [15]. The curves are as in Fig. 6.

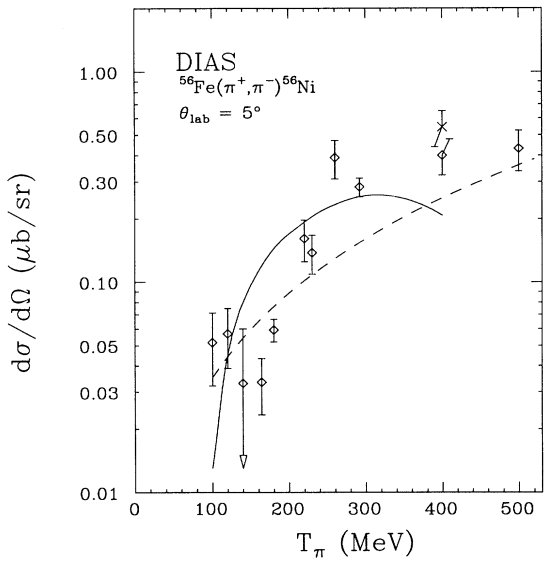

FIG. 8. Energy dependence of the DIAS in pion DCX in ^{56}Fe [10,16–18]. The solid curve is the NEWCHOP calculation of the excitation function; the dashed curve is the fitted k^2 dependence. The NEWCHOP calculation was performed with strengths fitted to the single charge-exchange data. The 400-MeV measurement done in this work was at 2° and has been plotted with a ×. This cross section has been renormalized to 5° using the NEWCHOP calculation shown in Fig. 4, and replotted with the same symbol as the other data. This was done to be able to compare the 400-MeV data with the other energies measured at 5°.

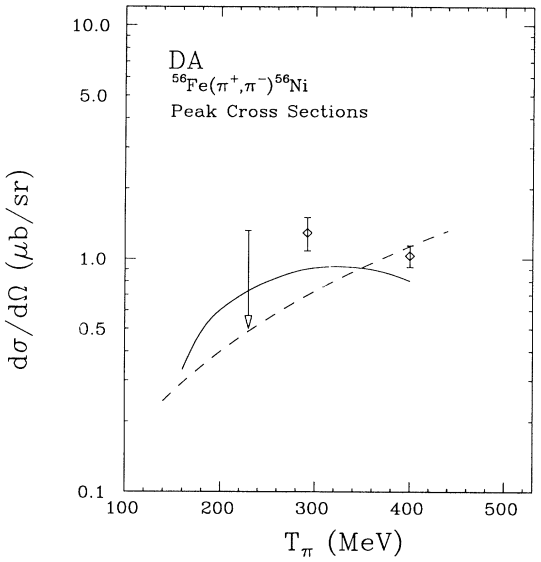

FIG. 9. Energy dependence of the DA in pion DCX on ^{56}Fe. The solid curve is the NEWCHOP calculation for this reaction; the dashed curve is the fitted k^2 dependence. The strength of the NEWCHOP calculation was found from fits to the single charge-exchange data. The 230-MeV upper limit is from a reanalysis of earlier data.

dependence, which continues to increase with energy.

The energy dependence of the DA is shown in Fig. 9; the 292-MeV point is from Ref. [6]. The solid line is the NEWCHOP calculation using the β's for the IAS and the GDR measured in SCX. The calculation matches the energy dependence of this state quite well, exhibiting a decrease in magnitude at higher energies. This is in contrast to the k^2 curve, which continues to increase. The absolute magnitude of the calculation also matches the data reasonably well. On the other hand, the DD calculations using the SCX distortions do not agree with the data. These calculations were done for the 0^+ and 2^+ components separately and summed. The energy dependence calculations for the DD are shown with the data (292-MeV point from Ref. [7]) in Fig. 10. Here, NEWCHOP results fall well below the data and do not predict the increase in cross section with energy. The

TABLE III. Peak centroids and widths of the photonuclear GDR previously measured on the slightly deformed nucleus ^{60}Ni [1].

E_x (MeV)	Γ (MeV)	σ (mb)
16.30	2.44	34.1
18.51	6.37	17.77

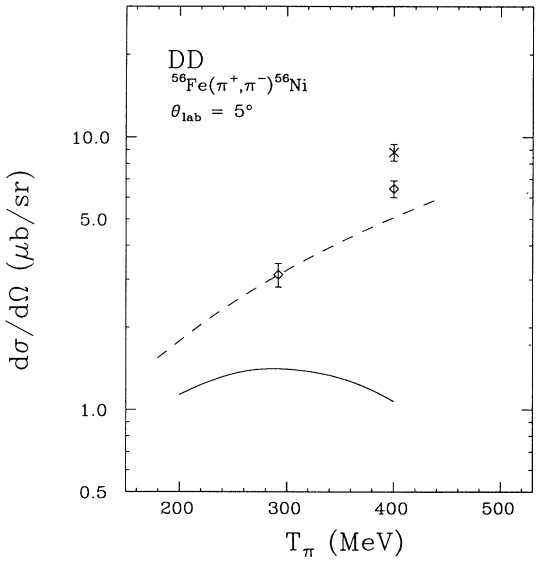

FIG. 10. Energy dependence of the DD observed in pion DCX on ^{56}Fe. The dashed curve is the fitted k^2 dependence; the solid curve is the NEWCHOP calculation for this reaction. The calculation was done using strengths found from fits to the SCX data. The 400-MeV measurement in this work was at 2° and has been plotted as a ×. This datum has been renormalized to 5° using the NEWCHOP calculations shown in Fig. 5, and replotted with the same symbol as the 292-MeV datum measured at 5° [7].

TABLE IV. Cross sections found fitting the DD as two peaks. The widths of the Lorentzian peak shapes were fixed at 9.0 MeV in the fittings.

Component	$-Q$ (MeV)	Γ (MeV)	$d\sigma/d\Omega$ (μb/sr)		
			2°	10°	20°
0^+	45.61 ± 0.64	9.0	4.96 ± 0.54	0.96 ± 0.21	0.57 ± 0.23
2^+	55.00 ± 0.69	9.0	3.27 ± 0.65	0.87 ± 0.24	2.43 ± 0.28

k^2 dependence, however, does predict the approximately correct energy dependence.

In the analysis of the DD it was found that the centroid of this peak changed with angle. At smaller angles the centroid was at 46 MeV, but at 20° the centroid was best fitted as 55 MeV. This change in excitation suggested that the DD region of the data would be better fitted as two peaks. One Lorentzian peak shape was fitted at the 2° centroid energy of 46 MeV and another peak at the 20° excitation of 55 MeV. These two peaks possess different angular distributions: The lower energy peak has a 0^+ shape and the higher peak a 2^+ shape.

The DD is a double excitation of the 1^- GDR and will be made up of 0^+ and 2^+ components. Splitting of the spin components of the DD can arise from different effects such as deformation, mixing, and configuration splitting. It has been noted that spin splitting due to mixing and configuration splitting would not be observable for such a broad resonance as the DD [8]. Deformation splitting of the GDR has been measured for ^{60}Ni, a nucleus comparable to ^{56}Fe. The photonuclear data on ^{60}Ni are listed in Table III [1]. The separation in energy of the J^π components that we observe for the DD is most probably due to deformation.

The DCX data were carefully fitted with two peaks having widths of 9 MeV each, to match the sum of the widths in the photonuclear data listed in Table III. The sum of the GDR widths was used as a first-order assumption. The results of these fits for all three angles, and after background subtraction, are shown in Fig. 11. The measured splitting from this fitting is 9.4 MeV. It has been theorized that the deformed DD would split into many components, having different J^π and strengths [19]. We are fitting the strongest two components and probably missing weaker components in between because of low statistics, thereby accounting for the large value of the splitting. The cross sections of the two peaks result-

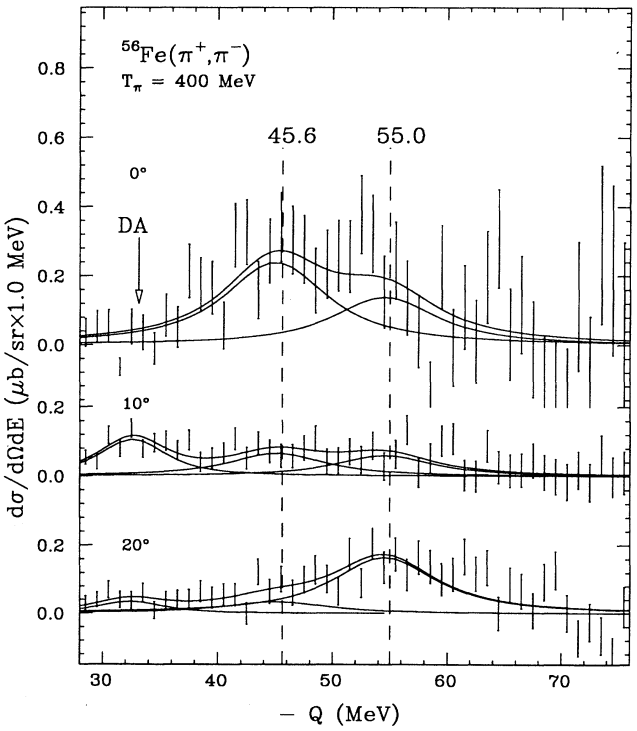

FIG. 11. Plot of the data in the dipole region, after background subtraction. The solid lines are fitted Lorentzian peak shapes. The centroid of the DD changes with angle, suggesting two resonances of different angular momentum. This region, fitted with two peaks, exhibits a 0^+ shape at 45.6 MeV and a 2^+ shape at 55.0 MeV.

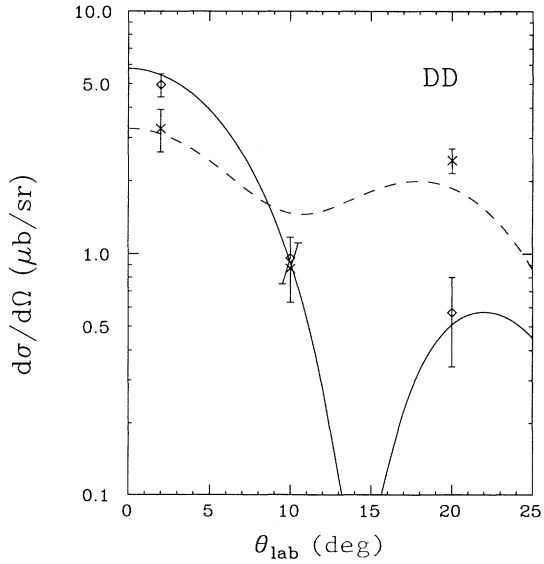

FIG. 12. Plot of cross sections measured when fitting the DD as two peaks. The circles are the 45.6-MeV, 0^+ component of the DD, and the ×'s are the 55.0-MeV, 2^+ member of the DD. The NEWCHOP calculation for the 0^+ is shown as a solid line; the 2^+ is the dashed line. These are the calculations described in the text multiplied by a factor of 5.9 to best fit the data. This fitting has a reduced χ^2 of 2.3.

ing from the fits are listed in Table IV, and the angular distributions are compared to NEWCHOP calculations in Fig. 12. The calculations were done for 0^+ and 2^+ states separately using the β parameters as found from SCX data. These were fitted to the DCX data and a factor of 5.88 ± 0.11 was found to best fit the data. The data are remarkably similar to the calculations, and show a good separation into these two different spin components.

SUMMARY

Data were measured on ^{56}Fe$(\pi^+,\pi^-)^{56}$Ni with T_π = 400 MeV at three angles 2°, 10°, and 20°. The angular distribution shapes of the data were analyzed to find the excitations and cross sections of the DIAS, DA, and the DD. Calculations were done with the coupled-channels distorted-wave code NEWCHOP fitting strengths to SCX data on ^{60}Ni, and compared to energy dependence of the DIAS, DA, and the DD. The magnitudes of these calculations agree with the data on the DIAS and the DA, but the DD calculations fall well below the measurements. The DD also shows evidence of spin splitting, and cross sections have been compared to calculations for the 0^+ and 2^+ components of this resonance.

ACKNOWLEDGMENTS

This work was supported by grants from the National Science Foundation and the Department of Energy.

[1] B. L. Berman and S. C. Fultz, Rev. Mod. Phys. **47**, 713 (1975), and references therein.
[2] A. Erell, J. Alster, J. Lichtenstadt, M. A. Moinester, J. D. Bowman, M. D. Cooper, F. Irom, H. S. Matis, E. Piasetzky, and U. Sennhauser, Phys. Rev. C **34**, 1822 (1986).
[3] F. Irom *et al.*, Phys. Rev. C **34**, 2231 (1986).
[4] S. Mordechai *et al.*, Phys. Rev. Lett. **60**, 408 (1988).
[5] S. Mordechai *et al.*, Phys. Rev. Lett. **61**, 531 (1988).
[6] S. Mordechai *et al.*, Phys. Rev. C **40**, 850 (1989).
[7] S. Mordechai, H. T. Fortune, J. M. O'Donnell, G. Lui, M. Burlein, A. H. Wuosmaa, S. Greene, C. L. Morris, N. Auerbach, S. H. Yoo, and C. F. Moore, Phys. Rev. C **41**, 202 (1990).
[8] J. M. O'Donnell, H. T. Fortune, and E. Rost, Phys. Rev. C **44**, 2426 (1991).
[9] A. L. Williams, Ph.D. thesis, University of Texas at Austin, Los Alamos Report No. LA-12209-T, 1991.
[10] P. A. Seidl *et al.*, Phys. Rev. C **42**, 1929 (1990).
[11] E. Rost, computer code CHOPIN (unpublished). The code has been modified by C. L. Morris to calculate pion charge-exchange reactions and renamed NEWCHOP.
[12] H. de Vries, C. W. de Jager, and C. de Vries, At. Data Nucl. Data Tables **36**, 494 (1987), and references therein.
[13] S. H. Rokni *et al.*, Phys. Lett. B **202**, 35 (1988).
[14] U. Shennhauser *et al.*, Phys. Rev. Lett. **51**, 1324 (1983).
[15] R. A. Loveman *et al.*, Phys. Rev. C **40**, 2710 (1989).
[16] R. Gilman *et al.*, Phys. Rev. C **35**, 1334 (1987).
[17] P. A. Seidl *et al.*, Phys. Rev. Lett. **50**, 1106 (1983).
[18] A. L. Williams, *et. al.*, Phys. Rev. C **44**, 2025 (1991).
[19] F. G. Scholtz and F. J. W. Hahne, Z. Phys. A **336**, 145 (1990).